Mining Unseen Classes via Regional Objectness: A Simple Baseline for Incremental Segmentation

Zekang Zhang¹*, Guangyu Gao¹†, Zhiyuan Fang¹, Jianbo Jiao², Yunchao Wei^{3,4}

School of Computer Science, Beijing Institute of Technology
 School of Computer Science, University of Birmingham

Abstract

Incremental or continual learning has been extensively studied for image classification tasks to alleviate *catastrophic forgetting*, a phenomenon that earlier learned knowledge is forgotten when learning new concepts. For class incremental semantic segmentation, such a phenomenon often becomes much worse due to the background shift, i.e., some concepts learned at previous stages are assigned to the background class at the current training stage, therefore, significantly reducing the performance of these old concepts. To address this issue, we propose a simple yet effective method in this paper, named Mining unseen Classes via Regional Objectness for Segmentation (MicroSeg). Our MicroSeg is based on the assumption that background regions with strong objectness possibly belong to those concepts in the historical or future stages. Therefore, to avoid forgetting old knowledge at the current training stage, our MicroSeg first splits the given image into hundreds of segment proposals with a proposal generator. Those segment proposals with strong objectness from the background are then clustered and assigned newly-defined labels during the optimization. In this way, the distribution characterizes of old concepts in the feature space could be better perceived, relieving the *catastrophic forgetting* caused by the background shift accordingly. Extensive experiments on Pascal VOC and ADE20K datasets show competitive results with state-of-the-art, well validating the effectiveness of the proposed MicroSeg. Code is available at https://github.com/zkzhang98/MicroSeg.

1 Introduction

Deep learning based methods have made significant achievements on various recognition tasks, while assuming the data distribution to be fixed or stable and the training samples are independently and identically distributed [18]. However, in practical scenarios, the data always presents a continuous stream without a stable distribution. Under these scenarios, the old knowledge will be easily interfered with or even totally forgotten by continuously acquiring new knowledge, which is generally considered to be *catastrophic forgetting* [3, 24, 28]. To tackle this problem, many approaches were proposed to incrementally learn new concepts over time but without forgetting old knowledge, especially for the classification task, *i.e.*, Class-Incremental Learning (CIL) [17, 19].

Meanwhile, Class-Incremental Semantic Segmentation (CISS), aiming to predict a pixel-wise mask for an image in CIL scenarios, is crucial for applications like autonomous driving and robotics.

³ WEI Lab, Institute of Information Science, Beijing Jiaotong University

⁴ Beijing Key Laboratory of Advanced Information Science and Network zkzhang1998@outlook.com

^{*}Work done during an internship at WEI Lab of Beijing Jiaotong University.

[†]Corresponding author.

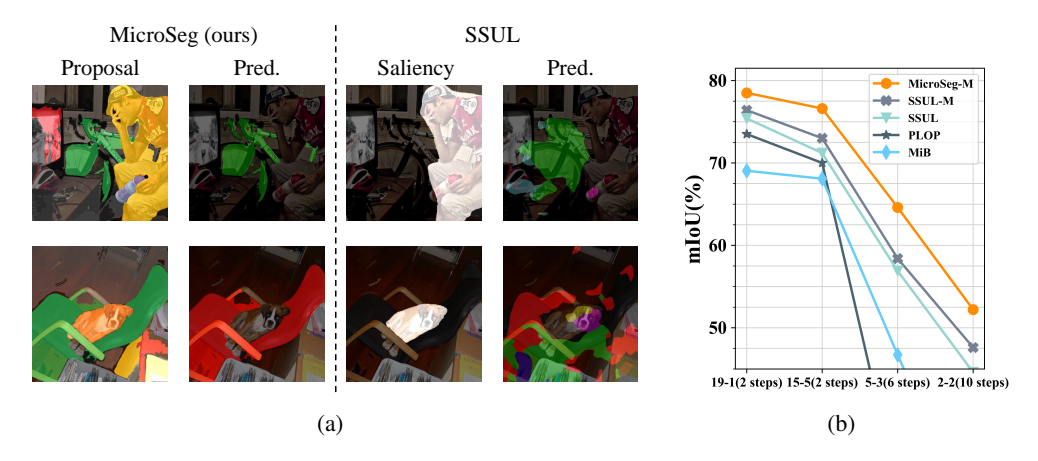


Figure 1: (a) Comparison of our proposed MicroSeg and the state-of-the-art SSUL [5]. Saliency detection only points out the most important area of an image, leaving the rest unseen classes result in semantic shift and lead to incorrect predictions. The proposed proposal-based approach attends each pixels within the sample, including both *things* and *stuff*. (b) Performance comparison of prior works when the number of incremental step increases (mIoU < 45% has been dropped out).

Nevertheless, besides *catastrophic forgetting of old concepts* in CIL, CISS involves an additional key issue of *background shift* in the image [4], making CISS rather challenging. Specifically, *background shift* means that the class of background (all other classes that are not learned at the moment) is shifting over the learning steps. As a result, such background shift will confuse the model and make it more difficult to distinguish different unseen classes, which generally include the true background (dummy) class, the historical classes, and future classes.

The problems of catastrophic forgetting and background shift in CISS have been studied in recent works [4, 5, 11]. MiB [4] proposed a distillation-based framework to address the background shift issue. PLOP [11] re-models the background labels with pseudo-labeling w.r.t. predictions of the old model for historical classes. However, these prior works did not particularly address the future classes issue that leads to background shift, while instead treating those future classes as background. These future classes will not only interfere with old knowledge due to catastrophic forgetting, but also be constantly introduced as current classes to be accurately identified. The state-of-the-art method SSUL [5] tried to address the future class issue by introducing an unknown class according to saliency detection. However, as shown in Fig. 1 (a), as saliency only highlights a few regions within an image, most unseen classes still remain in the background and result in background shift. As shown in Fig. 1 (b), with the number of incremental steps increasing, the performance of the aforementioned methods has a dramatic performance drop, suggesting that the background shift issue still apparently exists, especially for the challenging setting of more learning steps. Whereas for our approach (MicroSeg-M in Fig. 1 (b)), it outperforms prior works at each step. Furthermore, if considering the incremental learner lies in a lifelong learning process, the number of unseen classes would be infinite and diverse with endless learning steps. Thus, the unseen classes in each learning step become even more non-negligible, which interfere not only with maintaining concepts of historical classes, but also with the learning of current classes.

To address the above-mentioned issues in CISS, especially the unseen classes, we propose a simple yet effective approach for Mining unseen Classes via Regional Objectness for the Segmentation task (MicroSeg). MicroSeg first generates a set of segment proposals for input samples with a proposal generator. Each proposal is a binary mask pointing out a segment with strong objectness in an image. This mask is also class-agnostic and can generalize even to unseen categories. With the assumption of background regions with strong objectness belong to concepts either in the historical or future steps, the proposals from the background can be confidently clustered and re-modeled as unseen classes. Following that, proposal-based mask classification [8, 9] is applied to label each proposal with current classes and unseen classes. Moreover, to better cache the feature diversity in loose future classes into particular unseen classes, multiple sub-classes are explicitly defined and clustered according to a contrastive loss. As shown in Fig. 1 (a), the background shift issue gets alleviated with the discovery of unseen classes, showing the effectiveness of the proposed MicroSeg in reducing semantic ambiguity within categories.

Extensive experimental analysis on Pascal VOC2012 and ADE20K show the effectiveness and competitive performance of the proposed MicroSeg. MicroSeg consistently achieves higher performance across all benchmark datasets, on all incremental learning settings, e.g., an average of 3% improvements over the state-of-the-art method on Pascal VOC2012 and 2% on ADE20K. Particularly, MicroSeg outperforms prior works in the more challenging setting of long-term incremental scenarios, e.g., the performance gain of 6.2% on Pascal VOC 2012.

2 Related work

Class incremental learning (CIL). Class incremental learning (CIL) is incremental learning bound to classification tasks. Due to the catastrophic forgetting, some approaches consider CIL as a *trade-off* between defying forgetting and learning from new samples of a network. The earlier work to deal with catastrophic forgetting is mainly about parameter isolation [2, 23, 33–35, 40], which assigns isolated models parameters for each task, while the number of parameters will always grow without an upper bound with task increases. Replay-based approaches [10, 22, 30, 31, 36] were proposed by maintaining a sampler of data for future training. Later, regularization-based methods [1, 17, 19, 29, 41], such as knowledge distillation [15] appears, which rely on a teacher model for transferring knowledge of previous categories to current models.

Semantic segmentation. In semantic segmentation, deep models have achieved outstanding performance. FCN [21] and U-Net [32] replace fully connected layers with convolution layers to preserve the location information of pixels. The following methods [16, 25, 38, 39, 44] are mainly based on FCN and enlarge the perceptual field, making it more suitable for semantic segmentation tasks that require intensive annotation. DeepLab series methods [6, 7] contains an Atrous Spatial Pyramid Pooling (ASPP) for semantic segmentation using dilated convolution to capture multi-scale information. Meanwhile, MaskFormer [9] regards the semantic segmentation as a mask classification task and introduces the transformer [37] to obtain a better performance. Specifically, they first generate mask proposals and then perform mask classification with the queries generated by the transformer.

Class incremental semantic segmentation (CISS). Previous work has made attempts at semantic segmentation in incremental learning scenarios. Modeling-the-Background (MiB) [4] first clarifies the background shift in CISS, and proposed a distillation-based framework as in CIL. The subsequent work of Sparse and Disentangled Representations (SDR) [27] exploited a latent space to reduce forgetting, especially stored prototypes (class centroids) to recall the previous categories. Meanwhile, Douillard et al. [11] proposed the approach of PLOP to utilize the pseudo-label of the background pixels in the current step with the previously learned model as supervision. Furthermore, the SSUL [5] introduces an additional unknown class label to unseen objects in the background by an off-the-shelf saliency-map detector, preventing the model from forgetting by freezing model parameters.

3 Method

3.1 Problem Definition

We follow the common definition of Class Incremental Semantic Segmentation (CISS) as in the previous work [5, 11], but also give a more clear definition on the background class and unseen classes. In CISS, there are a series of incremental learning steps, as $t=1,\ldots,T$. Let \mathcal{D}_t denotes the dataset for the t_{th} learning step, and \mathcal{C}_t the class set of samples in dataset \mathcal{D}_t . For any pair $(\boldsymbol{x}_t, \boldsymbol{y}_t)$ within $\mathcal{D}_t, \boldsymbol{x}_t = \{\boldsymbol{x}_{t,i}\}_{i=1}^Q$ and $\boldsymbol{y}_t = \{\boldsymbol{y}_{t,i}\}_{i=1}^Q$ denote the input image and its ground-truth mask with Q pixels, respectively. Unlike previous approaches that specifically define a background class, we argue that in a lifelong incremental learning process with annotations of both stuff and thing, all pixels that not belong to current class will be learned in the future. Therefore, in each learning step, the class set can be expressed as $\mathcal{C}_t \cup \{c_u\}$, where \mathcal{C}_t denotes the classes to be learned currently, and c_u denotes a special class consisting of all the historical and future classes. c_u can also be considered as the background class from the perspective of each current learning step, and varies for each learning step, where the background shift lies.

The CISS model $f_{t,\theta}$ with parameters θ at the t_{th} learning step, aims at assigning each pixel of x_t with the probability for each class. The model $f_{t,\theta}$ includes a convolutional feature extractor and a

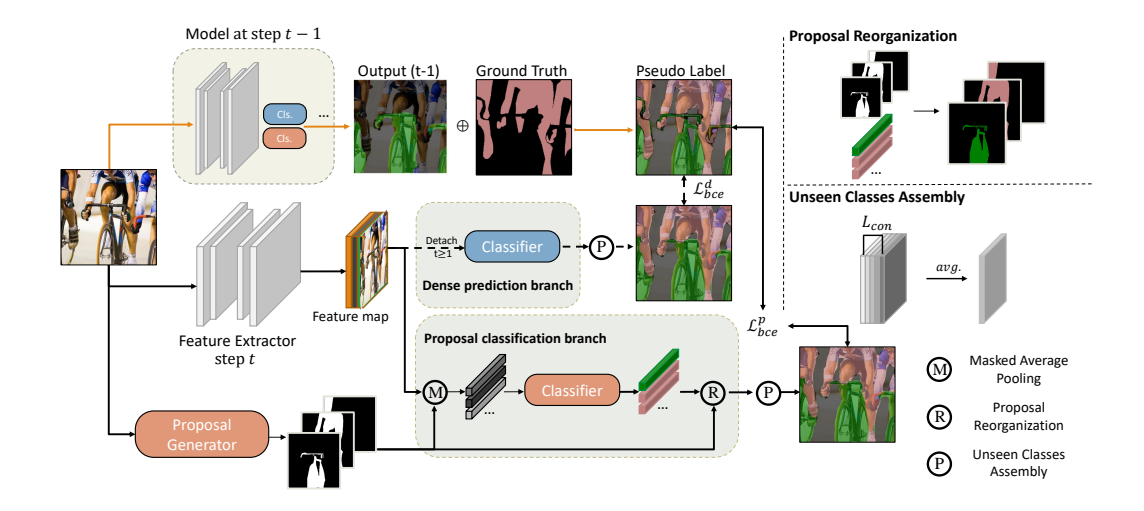


Figure 2: Overall architecture of the proposed MicroSeg.

classifier (to classify each category within the union of $C_{1:t} = \bigcup_{i=1}^t C_i$ and the unseen class c_u , *i.e.*, $C = C_{1:t} \cup c_u$). The model after the learning step t gives a prediction for all classes, within historical classes $C_{1:t-1}$. Specifically, the predicted result can be expressed as $\hat{y}_t = \arg\max_{c \in C} f_{t,\theta}^c(x)$. Thus, catastrophic forgetting happens due to the lack of historical and future classes supervision in C_t .

3.2 Overview of the MicroSeg

Fig. 2 illustrates the overall framework of our proposed method. We design a two-branch structure with the proposed Mining unseen Classes via Regional Objectness (Micro) mechanism. Given an input, the upper branch in Fig. 2 performs dense prediction over the whole image, while the lower branch splits it into segment proposals by proposal generator and classifies them into corresponding categories. In particular, we introduce the *micro mechanism* in the optimization process of both branches, to address the background shift issue.

Proposal generator. The proposal generator aims to generate a group of binary masks $P \in \{0,1\}^{N \times H \times W}$ where N is the number of proposals and H,W denote height and width. Unlike previous semantic segmentation methods, we split the task into class-agnostic proposal generation by Mask2Former [8] and proposal classification. In this study, all proposals are *disjoint*, and each pixel belongs to and only belongs to one proposal.

The dense prediction branch. The CISS model $f_{t,\theta}$ is composed of a feature extractor g_{t,θ_1} and a classifier h_{t,θ_2} . For convenience, we abbreviate $f_{t,\theta}$ as $f=h\circ g(\cdot)$. Note that the proposal classification branch and dense prediction branch share the same structure and parameters of $g(\cdot)$, but with different designs of $h(\cdot)$, i.e., $h_p(\cdot)$ and $h_d(\cdot)$. The dense prediction branch performs conventional semantic segmentation, i.e., $p_d=h_d(g(x))$ where p_d indicates the prediction scores (logits).

The proposal classification branch. In this branch, masked average pooling (MAP) [42] is used to generate prototype (centroid) $pr \in \mathbb{R}^{N \times C}$ of each proposal, where C is the number of channels of feature map. The logits $p \in \mathbb{R}^{N \times |\mathcal{C}|}$ of all proposals are generated by classifying pr, where $|\mathcal{C}| = |\mathcal{C}_{1:t} \cup \{c_u\}|$ denotes number of \mathcal{C} . Then p is reorganized to the original shape and the prediction scores are assigned accordingly. Formally, the proposal classification branch can be expressed as:

$$\boldsymbol{p}_{p} = Reg(h_{p}(MAP(g(\boldsymbol{x}), \boldsymbol{P})), \boldsymbol{P}), \tag{1}$$

where $Reg(\cdot)$ is the Proposal Reorganization shown in Fig. 2, and can be implemented by matrix multiplication, detailed in Supplementary Materials. The proposal classification branch focuses on objectness aggregation within a proposal, aiming at consistent representations in a particular proposal.

3.3 Mining Unseen Classes via Regional Objectness

Due to the background shift issue (*i.e.*, background class has unclear and unstable semantics during the training steps) mentioned above, the unseen class here refers to all the classes exclude the current foreground class. As mentioned in the observation in Sec. 1, this problem was not well explored in prior works, due to the ignorance of unseen classes. The proposed MicroSeg, on the other hand, can discover the unseen area with the proposal classification branch. Based on the assumption that background regions with strong objectness possibly belong to those concepts in the historical or future steps, we further remodel the supervision label and **mi**ning unseen classes via **r**egional **o**bjectness, namely, Micro mechanism. Mirco mechanism clusters proposals with strong objectness in unseen classes, and assigns them with new defined labels during the optimization.

Label remodeling. To capture the knowledge learned in the past learning step t-1, we extract the sample on $f_{t-1,\theta}$ during inference to get the pseudo label of mask \hat{y}_{t-1} and the corresponding prediction score map s_{t-1} . Formally:

$$\hat{\boldsymbol{y}}_{t-1} = \arg \max_{\mathcal{C}_{1:t-1}} f_{t-1,\boldsymbol{\theta}}(\boldsymbol{x}),$$

$$\boldsymbol{s}_{t-1} = \max_{\mathcal{C}_{1:t-1}} \sigma(f_{t-1,\boldsymbol{\theta}}(\boldsymbol{x})),$$
(2)

where $\sigma(\cdot)$ denotes Sigmoid function. With the ground truth mask $y_t = \{y_{t,i}\}$ in current step, we augment the supervision label $\tilde{y}_{t,i}$ of pixel i according to the following rules:

$$\tilde{\mathbf{y}}_{t,i} = \begin{cases}
\mathbf{y}_{t,i} & \text{where } \mathbf{y}_{t,i} \in \mathcal{C}_t \\
\hat{\mathbf{y}}_{t-1,i} & \text{where } \mathbf{y}_{t,i} = c_u \land \mathbf{s}_{t-1,i} > \tau , \\
c_{\hat{u}} & \text{others } (\text{ or } \mathbf{y}_{t,i} = c_u \setminus \mathcal{C}_{1:t-1})
\end{cases}$$
(3)

where τ represents a threshold for $\hat{y}_{t-1,i}$, $c_{\hat{u}}$ denotes future classes within the unseen class c_u , the symbol \wedge represents the co-taking of conditions and \setminus means the difference of the sets.

Micro mechanism. The micro mechanism is introduced to characterize the various semantics in unseen classes during the optimization and to alleviate the background shift issue. Even the future classes $c_{\hat{u}}$ include several classes of stuff or things, so we represent it as a set of K classes to better cache the feature diversity in those loose future classes. Formally, we represent $c_{\hat{u}} = \{c_{\hat{u},k}\}_{k=1}^K$, where each $c_{\hat{u},k}$ can be viewed as a cluster center of all the future classes. We impose both supervised and unsupervised constraints (detailed in Sec. 3.4) on $c_{\hat{u}}$ during the optimization. For the supervised part, the prediction scores of class $c_{\hat{u}}$ are assembled with the summary of the logits of $c_{\hat{u},k}$:

$$\boldsymbol{p}_{c_{\hat{u}}} = \sum_{k=1}^{K} \boldsymbol{p}_{k}(\boldsymbol{x}), \tag{4}$$

where $p_k(x) = f_{t,\theta}^{c_{\hat{u},k}}(x) \in \mathbb{R}^{H \times W}$ is the the prediction scores of class $c_{\hat{u},k}$. H and W denote the height and width of image samples respectively.

We argue that $c_{\hat{u}}$ captures more features with different spatial characteristics in unseen classes. This prevents potential classes from being incorrectly classified into historical classes $C_{1:t-1}$, which reduces the impact on historical knowledge and the collapse of class predictions. Besides, we equipped our method with the memory sampling strategy [5], resulting in *MicroSeg-M*. With rehearsal of samples from historical learning steps, catastrophic forgetting is alleviated significantly.

3.4 Objective Function

MicroSeg constrains the two branches via Binary Cross-Entropy (BCE) loss, calculated with augmented supervision label \tilde{y} from Eq. 3. Specifically, \mathcal{L}_{BCE} is defined as:

$$\mathcal{L}_{BCE} = -\frac{1}{|\mathcal{C}|} \frac{1}{Q} \sum_{l=1}^{|\mathcal{C}|} \sum_{i=1}^{Q} (\mathbb{1}[\tilde{\boldsymbol{y}}_{t,i} = c_l] \log(\sigma(\boldsymbol{p}_l^i)) + (1 - \mathbb{1}[\tilde{\boldsymbol{y}}_{t,i} = c_l]) \log(1 - \sigma(\boldsymbol{p}_l^i)))$$

$$-\frac{1}{Q} \sum_{i=1}^{Q} (\mathbb{1}[\tilde{\boldsymbol{y}}_{t,i} = c_{\hat{u}}] \log(\sigma(\boldsymbol{p}_{c_{\hat{u}}}^i)) + (1 - \mathbb{1}[\tilde{\boldsymbol{y}}_{t,i} = c_{\hat{u}}]) \log(1 - \sigma(\boldsymbol{p}_{c_{\hat{u}}}^i))),$$
(5)

where p_l^i means the predicted logits of the i_{th} pixel to the l_{th} class in \mathcal{C} , and $p_{c_{\hat{u}}}^i$ corresponds to $c_{\hat{u}}$ in Eq. 3. We note BCE loss of two branches as \mathcal{L}_{BCE}^p and \mathcal{L}_{BCE}^d .

Benefiting from the class-agnostic proposals, the proposal classification is able to discover the unseen classes in CIL. Meanwhile, the dense prediction is still helpful when the supervised label is complete, *i.e.*, the first learning step. The reason is that there is no historical class at the very initial learning step, where catastrophic forgetting is not yet happened. The dense prediction branch is also beneficial to learn a robust and versatile feature extractor on base classes, which is vital for the incremental settings, where historical samples are not available in the latter learning steps. The output of the whole model is from the proposal classification branch. The loss for this part is then defined as:

$$\mathcal{L}_{BCE} = \begin{cases} \mathcal{L}_{BCE}^p + \mathcal{L}_{BCE}^d & \text{if } t = 1\\ \mathcal{L}_{BCE}^p & \text{others} \end{cases}$$
 (6)

We also apply another constraint to enhance the unseen classes modeling, *i.e.*, the contrastive loss [13], to capture the diverse concepts in $c_{\tilde{u}}$:

$$\mathcal{L}_c = -\frac{1}{K} \sum_{i=1}^K \log \frac{\exp(\boldsymbol{p_i} \cdot \boldsymbol{p_i})}{\sum_{j=1}^K \exp(\boldsymbol{p_i} \cdot \boldsymbol{p_j})},$$
 (7)

where \cdot denotes the inner product. In Micro mechanism, we represent future classes $c_{\hat{u}}$ as explicitly-defined multiple sub-classes to better cache the feature diversity in those loose future classes. To avoid model degradation caused by $c_{\hat{u},k}$ characterizing the same features, we use unsupervised contrastive loss to force them to capture the diverse concepts, thus ensuring the effectiveness of the Micro mechanism.

Finally, the overall loss function is defined as below with a hyper-parameter λ to balance the two terms:

$$\mathcal{L} = \mathcal{L}_{BCE} + \lambda \cdot \mathcal{L}_c. \tag{8}$$

4 Experiments

4.1 Experimental Setups

Dataset. We have evaluated our approach on datasets of Pascal VOC 2012 [12] and ADE20K [43]. Pascal VOC 2012 contains 10,582 training images and 1449 validation images, with total of 20 foreground classes and one background class. ADE20K contains 20,210 training images and 2,000 validation images with 100 thing classes and 50 stuff classes.

Protocols. Following the conventions of previous work [5, 11], we evaluate our approach with *overlapped* experimental setup, which is more realistic and challenging than the *disjoint* setting studied by [4, 27]. For the *incremental scenario*, we apply the same representation as in the previous works [4, 27]. For example, the 15-1 scenario of Pascal VOC 2012 (including 20 foreground classes) takes 6 steps to train the model, *i.e.*, 15 classes are used in step 1 and one class for each step in steps 2 to 6. More details of protocols are shown in the supplementary materials.

Implementation details. Following the common practice [4, 5, 27], we use DeepLabv3 [6] and ResNet-101 [14] pretrained on ImageNet as the segmentation network, and the output stride is 16. We train the network using the SGD with a learning rate of 10^{-2} on Pascal VOC2012, and 5×10^{-3} for all steps on ADE20K. The momentum and weight decay are 0.9 and 10^{-4} on both datasets. The batch size is 16 for Pascal VOC 2012, and 12 for ADE20K. Data augmentation from [11] is applied to all the images. MicroSeg freezes the parameters of the feature extractor in the learning steps $t \ge 1$, following [5]. Our experiments are implemented with PyTorch on two NVIDIA GeForce RTX 3090 GPUs. We choose Mask2Former [8] pre-trained on MS-COCO [20] to generate N = 100 class-agnostic proposals. Note that, for fair comparisons, the proposal generator is **not** fine-tuned on any benchmark dataset. The setting of Micro mechanism is K = 5 for Pascal VOC 2012 and K = 1 for ADE20K. Thus, all pixels of samples in ADE20K can be potential foreground. Hyper-parameters $\tau = 0.7$ and $\lambda = 1$ are set for all experiments. With the same setting of memory sampling strategy as [5], we set the $|\mathcal{M}| = 100$ for Pascal VOC 2012 and $|\mathcal{M}| = 300$ for ADE20K to evaluate MicroSeg-M. More details are shown in the supplementary materials.

Table 1: Comparison with state-of-the-art meth	ods on Pascal VOC 2012.
--	-------------------------

Method	VOC	10-1 (11	steps)	VOC	2-2 (10	steps)	VOC	15-1 (6	steps)	VOC	5-3 (6	steps)	VOC	19-1 (2	steps)	VOC	15-5 (2	steps)
Method	0-10	11-20	all	0-2	2-18	all	0-15	16-20	all	0-5	6-20	all	0-19	20	all	0-15	16-20	all
LwF-MC [19]	4.7	5.9	4.9	3.5	4.7	4.5	6.4	8.4	6.9	20.9	36.7	24.7	64.4	13.3	61.9	58.1	35.0	52.3
ILT [26]	7.2	3.7	5.5	5.8	5.0	5.1	8.8	8.0	8.6	22.5	31.7	29.0	67.8	10.9	65.1	67.1	39.2	60.5
MiB [4]	12.3	13.1	12.7	41.1	23.4	25.9	34.2	13.5	29.3	57.1	42.6	46.7	71.4	23.6	69.2	76.4	50.0	70.1
SDR [27]	32.1	17.0	24.9	13.0	5.1	6.2	44.7	21.8	39.2	12.1	6.5	8.1	69.1	32.6	67.4	57.4	52.6	69.9
PLOP [11]	44.0	15.5	30.5	24.1	11.9	13.7	65.1	21.1	54.6	17.5	19.2	18.7	75.4	37.4	73.5	75.7	51.7	70.1
SSUL[5]	71.3	46.0	59.3	62.4	42.5	45.3	77.3	36.6	67.6	72.4	50.7	56.9	77.7	29.7	75.4	77.8	50.1	71.2
SSUL-M[5]	74.0	53.2	64.1	58.8	45.8	47.6	78.4	49.0	71.4	71.3	53.2	58.4	77.8	49.8	76.5	78.4	55.8	73.0
MicroSeg (Ours)	72.6	48.7	61.2	61.4	40.6	43.5	80.1	36.8	69.8	77.6	59.0	64.3	78.8	14.0	75.7	80.4	52.8	73.8
MicroSeg-M (Ours)	77.2	57.2	67.7	60.0	50.9	52.2	81.3	52.5	74.4	74.8	60.5	64.6	79.3	62.9	78.5	82.0	59.2	76.6
Joint	82.1	79.6	80.9	76.5	81.6	80.9	82.7	75.0	80.9	81.4	80.7	80.9	81.0	79.1	80.9	82.7	75.0	80.9

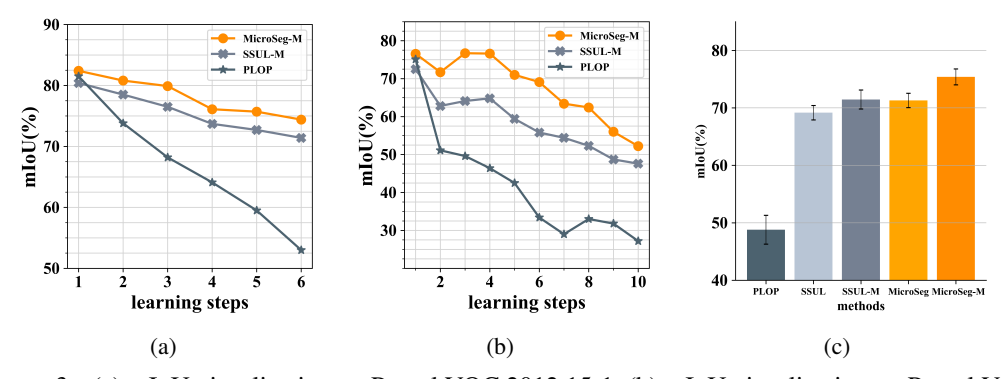


Figure 3: (a) mIoU visualization on Pascal VOC 2012 15-1, (b) mIoU visualization on Pascal VOC 2012 2-2, (c) mIoU on Pascal VOC 2012 in scenario 15-1, averaged over 20 different training orders.

Baselines. We evaluate our MicroSeg and MicroSeg-M, with the comparisons with some classical methods in CIL (*e.g.*, Lwf-MC [19] and ILT [26]), as well as the state-of-the-art methods in CISS, including MiB [4], SDR [27], PLOP [11], and SSUL [5]. For the methods of CIL, we applied them to each experimental setup of CISS. We use the commonly used mean Intersection-over-Union (mIoU) as the evaluation metric for all the experimental evaluation and comparisons. In our experiment, the result of each experiment setting shows in three columns, *i.e.*, mIoU of classes learned in learning step t=1 (base classes), in $t \geq 2$ (novel classes), and all classes to now, respectively. Besides comparing with prior methods, we also provides the experimental results of *joint* training, *i.e.*, training all classes offline. This setting is usually regarded as an upper bound of corresponding incremental scenario [4, 19].

4.2 Experimental Results

Experiments on Pascal VOC 2012. Besides the widely discussed scenarios of 19-1, 15-1, and 15-5 in previous works, we verified the performance of MicroSeg in several more challenging incremental scenarios, *e.g.*, scenarios of 5-3 (6 steps), 10-1 (11 steps), 2-2 (10 steps). These long-term incremental scenarios is more meaningful, and closer to situations in reality. Tab. 1 shows the final results after all learning steps in each incremental scenario. From the experiments, we can see that our approach has a very clear advantage over previous methods for all incremental scenarios. Even in the without-memory setting, MicroSeg shows performances over the state-of-the-art methods in almost all incremental scenarios. MicroSeg is obviously superior to SSUL with memory-free by the mIoU improvements of 2% to 3%, in the short-term incremental scenarios, *e.g.*, 19-1 and 15-5. While for the long-term scenarios, MicroSeg outperforms SSUL by a wider margin of up to over 7% improvement on mIoU. Not only that, MicroSeg-M (*i.e.*, MicroSeg with memory sampling of past samples) further strengthens the performances, and undoubtedly outperforms all prior methods in all scenarios.

Meanwhile, Fig. 3 (a) shows the change of average mIoU for all past classes under the scenarios of 15-1, with the training step progressing. In the first step, the performances of all methods are similar, but the mIoU starts to decrease as the learning steps increase because of the forgetting of the past classes. However, the mIoU of the previous work drops significantly, while MicroSeg effectively slows down the drop. By ensuring similar semantic segmentation capabilities to previous work, it demonstrates that MicroSeg exactly benefits incremental learning and outperforms prior works.

Table 2: Comparison with state-of-the-art methods on ADE20K.

Method	ADE 0-100	100-5 (11 s	teps)	ADE 0-100	100-10 (6 s 101-150	teps)	ADE 0-100	100-50 (2 s	teps)	ADE 0-50	50-50 (3 s	steps)
ILT [26]	0.1	1.3	0.5	0.1	3.1	1.1	18.3	14.4	17.0	3.5	12.9	9.7
MiB [4]	36.0	5.7	26.0	38.2	11.1	29.2	40.5	17.2	32.8	45.6	21.0	29.3
PLOP [11]	39.1	7.8	28.8	40.5	13.6	31.6	41.9	14.9	32.9	48.8	21.0	30.4
SSUL[5]	39.9	17.4	32.5	40.2	18.8	33.1	41.3	18.0	33.6	48.4	20.2	29.6
SSUL-M[5]	42.9	17.8	34.6	42.9	17.7	34.5	42.8	17.5	34.4	49.1	20.1	29.8
MicroSeg (Ours)	40.4	20.5	33.8	41.5	21.6	34.9	40.2	18.8	33.1	48.6	24.8	32.9
MicroSeg-M (Ours)	43.6	22.4	36.6	43.7	22.2	36.6	43.4	20.9	35.9	49.8	22.0	31.4
Joint	43.8	28.9	38.9	43.8	28.9	38.9	43.8	28.9	38.9	50.7	32.8	38.9

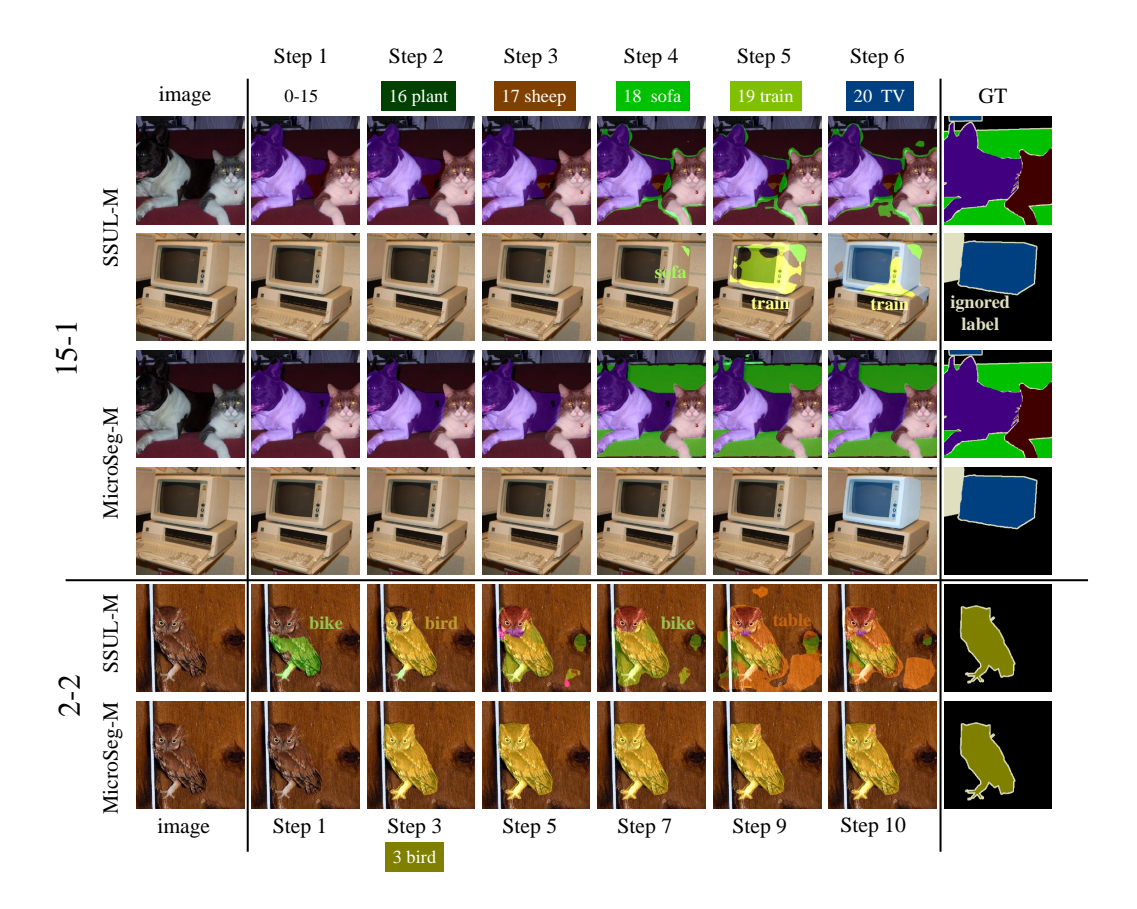


Figure 4: Qualitative analysis of MicroSeg on Pascal VOC 2012. Color-shaded boxes with semantic category and its index indicate the learned class during the corresponding step.

Fig. 3 (b) shows the similar analysis on the long-term scenario of 2-2. The effect of MicroSeg has shown a more significant advantage in such more challenging settings. Fig. 3 (c) shows the performance of MicroSeg with 20 random learning orders of 15-1 incremental scenario. Compared with prior approaches, our approach performs a better result with lower variance. The result illustrates that the robustness of our approach with various task settings outperforms prior methods.

Experiments on ADE20K. On the ADE20K dataset, we have provided experimental results with multiple incremental scenarios, which have various numbers of learning steps, and we extensively compared MicroSeg with prior methods in these setting. In Tab. 2, as in the case of Pascal VOC 2012, our MicroSeg has achieved a compelling enough performance without any samples sampling memory cost. Moreover, our MicroSeg-M extends this advantage and outperforms the previous state-of-the-art on all incremental scenarios. Further, the performance of our approach is very close to the offline training on base classes, and has a significant improvement to prior works on novel classes.

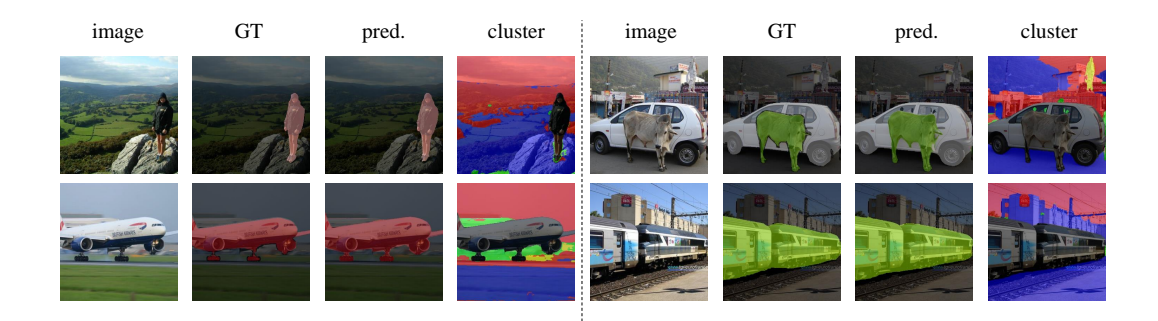


Figure 5: Qualitative performance of the proposed Micro mechanism. The first and second columns are sampled input images and ground truth. The third column shows the predictions of the last learning step. For the last column, distinct colors denotes different clusters of *unseen class*, *i.e.*, $c_{\hat{u},k}$ as mentioned in Sec. 3.3.

Qualitative analysis of MicroSeg. Fig. 4 shows qualitative analysis of our approach compared with SSUL-M, the current state-of-the-art method. Results are visualized of each learning step on multiple incremental scenarios of Pascal VOC 2012. First, we evaluated the typical scenario of 15-1 with a large number of base classes, to assess the plasticity of the model, *i.e.*, the ability to learn new classes. Regarding the samples set of {dog, cat, sofa} (the first and third rows), {dog, cat} belongs to the base classes while {sofa} is learnt in step 4. In contrast to SSUL-M, MicroSeg-M extract the feature of {sofa} well, and performs a complete segmentation of the novel class sofa. The other samples set (the second and fourth rows) is an image of TV (learned in the last learning step). The visualization indicated that, starting from step 4, SSUL-M tends to segment the images incorrectly into current foreground classes, *i.e.*, sofa and train, which are similar only in low-level semantic features (e.g., similar square shapes). Our approach, on the other hand, better learns the semantic features of the novel class by regional objectness, avoids the wrong segmentation, and segments it correctly and completely after learning the class TV.

We further evaluate the model stability (*i.e.*, ability to maintain old knowledge while learning new concepts) on the more challenging long-term scenario of 2-2. First SSUL-M incorrectly classifies *bird* in the image as *bike* at step 1 before learning *bird*. After learning class *bird*, SSUL-M products an acceptable result in step 3. However, in the subsequent learning step, the prediction results become more and more chaotic. Meanwhile, our MicroSeg has stronger stability, even in a long-term incremental scenario. MicroSeg maintains consistent results in multiple steps, and mitigates the negative effect of noise on the prediction with Micro mechanism.

Qualitative analysis of the Micro mechanism Fig. 5 shows the qualitative results of the proposed Micro mechanism. For the 'cluster' column, distinct colors denotes different clusters of *unseen class*, *i.e.*, $c_{\hat{u},k}$ motioned in Sec. 3.3. It can be seen from the figure, the background of samples are clustered well and reasonably with the Micro mechanism, even without supervision by ground truth. The mining of the unseen class not only mitigates the impact of the historical knowledge issue, but also benefits learning new concepts.

4.3 Ablation Study

Effect of components in MicroSeg.

Tab. 3 shows the contributions of two components of our approach, including proposal classification branch and Micro mechanism. The first row refers to the baseline and the last row stands for MicroSeg. The ablation studies are done on VOC 15-1. We will analyze them separately. The proposal classification branch improves the mIoU in the base class and the novel class, thus leading to an overall performance improvement.

Table 3: Ablation study of components in the proposed method on VOC 15-1, with DP (dense prediction branch), Proposal (proposal classification branch), and Micro (Micro mechanism). Numbers in brackets are the improvements over baseline (the first row).

			V	OC 15-1	(6 tasks)
DP	Proposal	Micro	0-15	16-20	all
√	Х	Х	69.1	14.0	56.0
1	×	✓	76.8	31.2	65.9 (+9.9)
1	✓	X	77.8	32.2	66.9 (+10.9)
✓	✓	✓	80.1	36.8	69.8 (+13.8)

The usage of proposal classification branch increases both stability and plasticity, which are the most critical elements in incremental learning. As for Micro mechanism, observe the first and second rows of the table, the application of Micro mechanism decreases the influence of background shift, significantly improves the result. Due to the design of the Micro mechanism, the model generates more reasonable augmented labels and decreases the influence of background shift, strengthening the ability for acquiring novel classes and maintaining historical concepts. Finally, by combining the two components, MicroSeg can get better performance, 13.8% over the baseline.

Effect of dense prediction branch. Tab. 4 shows the effect of dense prediction branch. As we discussed in Sec. 3.4, this branch is only used when learning step t=1. Hence, the constraint of dense prediction is only applied when the model is trained on the base classes. The result shows the comparison between the experiment of applying proposal classification branch only and using both branches. It can be observed that at the first learning step, dense prediction

Table 4: Ablation study of the dense prediction branch on VOC 15-1. DP: dense prediction branch, Proposal: proposal classification branch.

Setting	step=1 base	0-15	step=6 16-20	all
Proposal	82.2	77.6	28.0	65.8
Proposal+DP	83.3	80.1	36.8	69.8

branch benefits the training on base classes. When all training steps are done, mIoU of novel classes is significantly improved. Dense prediction branch enables the model to be trained better on the base classes. Since MicroSeg applies remodeled labels composed of pseudo label, the quality of predictions of past classes becomes vital to the results. Thus, it increases the performance of the novel classes by improving the reliability of the remodeled label.

Ablation of hyper-parameters. Tab. 5 illustrates the influence of hyper-parameters: the number of future classes K and threshold τ in label-remodeling. The results show that in most cases, our approach is not as sensitive to hyper-parameters.

Table 5: Search of hyper-parameters: the number of future classes K, and threshold τ in label-remodeling. All experiment are conducted on VOC 15-1.

						16-20	
1	78.6	30.9	67.2	0.1	79.7	30.7 31.3 33.1 36.8 32.5	68.3
3	79.7	34.0	68.8	0.3	81.1	31.3	69.2
5	80.1	36.8	69.8	0.5	80.8	33.1	69.4
7	80.4	32.8	69.1	0.7	80.1	36.8	69.8
9	80.1	33.1	68.9	0.9	80.0	32.5	68.7

5 Conclusions

In this study, we propose an effective method, MicroSeg, aiming at class incremental semantic segmentation problems by mining unseen classes via regional objectness. We first introduce proposals into class incremental semantic segmentation, and design a proposal-guided segmentation branch. To tackle background shift, we propose Micro mechanism, clustering and remodeling unseen classes, to capture diverse category features. Experiments demonstrate the effectiveness of our method. MicroSeg and MicroSeg-M achieve remarkable performance, especially on long-term incremental scenarios, outperforming prior state-of-the-art class incremental semantic segmentation methods.

Limitations and societal impact. Although our proposed Micro mechanism effectively mitigates background shift, catastrophic forgetting still exists as the learning step increases. As a simple baseline, we hope our work to inspire following-up research towards more challenging scenarios in incremental learning, *e.g.*, few base classes and long-term settings.

Acknowledgment. This work was supported in part by the National Key R&D Program of China (No.2021ZD0112100), the National Natural Science Foundation of China (No. 61972036), the Fundamental Research Funds for the Central Universities (No. K22RC00010).

References

- [1] Rahaf Aljundi, Francesca Babiloni, Mohamed Elhoseiny, Marcus Rohrbach, and Tinne Tuytelaars. Memory aware synapses: Learning what (not) to forget. In *Proc. European Conference on Computer Vision*, pages 139–154, 2018.
- [2] Rahaf Aljundi, Punarjay Chakravarty, and Tinne Tuytelaars. Expert gate: Lifelong learning with a network of experts. In *Proc. IEEE Conference on Computer Vision and Pattern Recognition*, pages 3366–3375, 2017.
- [3] Gert Cauwenberghs and Tomaso Poggio. Incremental and decremental support vector machine learning. *Advances in neural information processing systems*, 13, 2000.
- [4] Fabio Cermelli, Massimiliano Mancini, Samuel Rota Bulo, Elisa Ricci, and Barbara Caputo. Modeling the background for incremental learning in semantic segmentation. In *Proc. IEEE Conference on Computer Vision and Pattern Recognition*, pages 9233–9242, 2020.
- [5] Sungmin Cha, YoungJoon Yoo, Taesup Moon, et al. Ssul: Semantic segmentation with unknown label for exemplar-based class-incremental learning. *Advances in neural information processing systems*, 34, 2021.
- [6] Liang-Chieh Chen, George Papandreou, Iasonas Kokkinos, Kevin Murphy, and Alan L Yuille. Deeplab: Semantic image segmentation with deep convolutional nets, atrous convolution, and fully connected crfs. *IEEE Transactions on Pattern Recognition and Machine Intelligence*, 40(4):834–848, 2017.
- [7] Liang-Chieh Chen, George Papandreou, Florian Schroff, and Hartwig Adam. Rethinking atrous convolution for semantic image segmentation. *arXiv preprint arXiv:1706.05587*, 2017.
- [8] Bowen Cheng, Ishan Misra, Alexander G Schwing, Alexander Kirillov, and Rohit Girdhar. Masked-attention mask transformer for universal image segmentation. *arXiv* preprint *arXiv*:2112.01527, 2021.
- [9] Bowen Cheng, Alexander G. Schwing, and Alexander Kirillov. Per-pixel classification is not all you need for semantic segmentation. *Advances in neural information processing systems*, 34, 2021.
- [10] Matthias De Lange and Tinne Tuytelaars. Continual prototype evolution: Learning online from non-stationary data streams. In *Proc. IEEE International Conference on Computer Vision*, pages 8250–8259, 2021.
- [11] Arthur Douillard, Yifu Chen, Arnaud Dapogny, and Matthieu Cord. Plop: Learning without forgetting for continual semantic segmentation. In *Proc. IEEE Conference on Computer Vision and Pattern Recognition*, pages 4040–4050, 2021.
- [12] Mark Everingham, Luc Van Gool, Christopher KI Williams, John Winn, and Andrew Zisserman. The pascal visual object classes (voc) challenge. *International Journal on Computer Vision*, 88(2):303–338, 2010.
- [13] Kaiming He, Haoqi Fan, Yuxin Wu, Saining Xie, and Ross Girshick. Momentum contrast for unsupervised visual representation learning. In *Proc. IEEE Conference on Computer Vision and Pattern Recognition*, pages 9729–9738, 2020.
- [14] Kaiming He, Xiangyu Zhang, Shaoqing Ren, and Jian Sun. Deep residual learning for image recognition. In *Proc. IEEE Conference on Computer Vision and Pattern Recognition*, pages 770–778, 2016.
- [15] Geoffrey Hinton, Oriol Vinyals, Jeff Dean, et al. Distilling the knowledge in a neural network. *arXiv preprint arXiv:1503.02531*, 2(7), 2015.
- [16] Zilong Huang, Xinggang Wang, Lichao Huang, Chang Huang, Yunchao Wei, and Wenyu Liu. Ccnet: Criss-cross attention for semantic segmentation. In *Proc. IEEE International Conference on Computer Vision*, pages 603–612, 2019.

- [17] Heechul Jung, Jeongwoo Ju, Minju Jung, and Junmo Kim. Less-forgetting learning in deep neural networks. *arXiv preprint arXiv:1607.00122*, 2016.
- [18] Yann LeCun, Yoshua Bengio, and Geoffrey Hinton. Deep learning. *nature*, 521(7553):436–444, 2015.
- [19] Zhizhong Li and Derek Hoiem. Learning without forgetting. *IEEE Transactions on Pattern Recognition and Machine Intelligence*, 40(12):2935–2947, 2017.
- [20] Tsung-Yi Lin, Michael Maire, Serge Belongie, James Hays, Pietro Perona, Deva Ramanan, Piotr Dollár, and C Lawrence Zitnick. Microsoft coco: Common objects in context. In *Proc. European Conference on Computer Vision*, pages 740–755, 2014.
- [21] Jonathan Long, Evan Shelhamer, and Trevor Darrell. Fully convolutional networks for semantic segmentation. In *Proc. IEEE Conference on Computer Vision and Pattern Recognition*, pages 3431–3440, 2015.
- [22] David Lopez-Paz and Marc'Aurelio Ranzato. Gradient episodic memory for continual learning. Advances in neural information processing systems, 30, 2017.
- [23] Arun Mallya and Svetlana Lazebnik. Packnet: Adding multiple tasks to a single network by iterative pruning. In *Proc. IEEE Conference on Computer Vision and Pattern Recognition*, pages 7765–7773, 2018.
- [24] Michael McCloskey and Neal J Cohen. Catastrophic interference in connectionist networks: The sequential learning problem. In *Psychology of learning and motivation*, volume 24, pages 109–165. Elsevier, 1989.
- [25] Sachin Mehta, Mohammad Rastegari, Anat Caspi, Linda Shapiro, and Hannaneh Hajishirzi. Espnet: Efficient spatial pyramid of dilated convolutions for semantic segmentation. In *Proc. European Conference on Computer Vision*, pages 552–568, 2018.
- [26] Umberto Michieli and Pietro Zanuttigh. Incremental learning techniques for semantic segmentation. In *Proc. IEEE International Conference on Computer Vision Workshops*, pages 0–0, 2019.
- [27] Umberto Michieli and Pietro Zanuttigh. Continual semantic segmentation via repulsion-attraction of sparse and disentangled latent representations. In *Proc. IEEE Conference on Computer Vision and Pattern Recognition*, pages 1114–1124, 2021.
- [28] Robi Polikar, Lalita Upda, Satish S Upda, and Vasant Honavar. Learn++: An incremental learning algorithm for supervised neural networks. *IEEE transactions on systems, man, and cybernetics, part C (applications and reviews)*, 31(4):497–508, 2001.
- [29] Amal Rannen, Rahaf Aljundi, Matthew B Blaschko, and Tinne Tuytelaars. Encoder based lifelong learning. In *Proc. IEEE International Conference on Computer Vision*, pages 1320–1328, 2017.
- [30] Sylvestre-Alvise Rebuffi, Alexander Kolesnikov, Georg Sperl, and Christoph H Lampert. icarl: Incremental classifier and representation learning. In *Proc. IEEE Conference on Computer Vision and Pattern Recognition*, pages 2001–2010, 2017.
- [31] David Rolnick, Arun Ahuja, Jonathan Schwarz, Timothy Lillicrap, and Gregory Wayne. Experience replay for continual learning. *Advances in neural information processing systems*, 32, 2019.
- [32] Olaf Ronneberger, Philipp Fischer, and Thomas Brox. U-net: Convolutional networks for biomedical image segmentation. In *Proc. International Conference on Medical Image Computing and Computer-Assisted Intervention*, pages 234–241, 2015.
- [33] Amir Rosenfeld and John K Tsotsos. Incremental learning through deep adaptation. *IEEE Transactions on Pattern Recognition and Machine Intelligence*, 42(3):651–663, 2018.

- [34] Andrei A Rusu, Neil C Rabinowitz, Guillaume Desjardins, Hubert Soyer, James Kirkpatrick, Koray Kavukcuoglu, Razvan Pascanu, and Raia Hadsell. Progressive neural networks. arXiv preprint arXiv:1606.04671, 2016.
- [35] Joan Serra, Didac Suris, Marius Miron, and Alexandros Karatzoglou. Overcoming catastrophic forgetting with hard attention to the task. In *Proc. International Conference on Machine Learning*, pages 4548–4557, 2018.
- [36] Hanul Shin, Jung Kwon Lee, Jaehong Kim, and Jiwon Kim. Continual learning with deep generative replay. *Advances in neural information processing systems*, 30, 2017.
- [37] Ashish Vaswani, Noam Shazeer, Niki Parmar, Jakob Uszkoreit, Llion Jones, Aidan N. Gomez, Lukasz Kaiser, and Illia Polosukhin. Attention is all you need. *Advances in neural information processing systems*, 30, 2017.
- [38] Panqu Wang, Pengfei Chen, Ye Yuan, Ding Liu, Zehua Huang, Xiaodi Hou, and Garrison Cottrell. Understanding convolution for semantic segmentation. In *Proc. IEEE/CVF Winter Conference on Applications of Computer Vision*, pages 1451–1460, 2018.
- [39] Huikai Wu, Junge Zhang, Kaiqi Huang, Kongming Liang, and Yizhou Yu. Fastfcn: Rethinking dilated convolution in the backbone for semantic segmentation. *arXiv* preprint *arXiv*:1903.11816, 2019.
- [40] Ju Xu and Zhanxing Zhu. Reinforced continual learning. Advances in neural information processing systems.
- [41] Junting Zhang, Jie Zhang, Shalini Ghosh, Dawei Li, Serafettin Tasci, Larry Heck, Heming Zhang, and C-C Jay Kuo. Class-incremental learning via deep model consolidation. In *Proc. IEEE/CVF Winter Conference on Applications of Computer Vision*, pages 1131–1140, 2020.
- [42] Xiaolin Zhang, Yunchao Wei, Yi Yang, and Thomas S Huang. Sg-one: Similarity guidance network for one-shot semantic segmentation. *IEEE Transactions on Cybernetics*, 50(9):3855– 3865, 2020.
- [43] Bolei Zhou, Hang Zhao, Xavier Puig, Sanja Fidler, Adela Barriuso, and Antonio Torralba. Scene parsing through ade20k dataset. In *Proc. IEEE Conference on Computer Vision and Pattern Recognition*, pages 633–641, 2017.
- [44] Zhen Zhu, Mengde Xu, Song Bai, Tengteng Huang, and Xiang Bai. Asymmetric non-local neural networks for semantic segmentation. In *Proc. IEEE International Conference on Computer Vision*, pages 593–602, 2019.

Checklist

- 1. For all authors...
 - (a) Do the main claims made in the abstract and introduction accurately reflect the paper's contributions and scope? [Yes] We introduce the main claims of our study in the Abstract and Introduction.
 - (b) Did you describe the limitations of your work? [Yes] We discuss the limitations and future work in Conclusions.
 - (c) Did you discuss any potential negative societal impacts of your work? [Yes] We discuss societal impact in Conclusions.
 - (d) Have you read the ethics review guidelines and ensured that your paper conforms to them? [Yes] We read and obey them faithfully.
- 2. If you are including theoretical results...
 - (a) Did you state the full set of assumptions of all theoretical results? [N/A]
 - (b) Did you include complete proofs of all theoretical results? [N/A]
- 3. If you ran experiments...
 - (a) Did you include the code, data, and instructions needed to reproduce the main experimental results (either in the supplemental material or as a URL)? [Yes] Code and instructions are included in Supplement materials.
 - (b) Did you specify all the training details (e.g., data splits, hyperparameters, how they were chosen)? [Yes] Training details are described in Experiments.
 - (c) Did you report error bars (e.g., with respect to the random seed after running experiments multiple times)? [Yes] We provide experimental results of evaluating our method with twenty random category orders.
 - (d) Did you include the total amount of compute and the type of resources used (e.g., type of GPUs, internal cluster, or cloud provider)? [Yes] Computing resources are described in Implementation Details, in the section of Experiments.
- 4. If you are using existing assets (e.g., code, data, models) or curating/releasing new assets...
 - (a) If your work uses existing assets, did you cite the creators? [Yes] The proposal generator in our method is based on mask2former.
 - (b) Did you mention the license of the assets? [N/A]
 - (c) Did you include any new assets either in the supplemental material or as a URL? [Yes]
 - (d) Did you discuss whether and how consent was obtained from people whose data you're using/curating? [Yes] The datasets we used in our work are open source.
 - (e) Did you discuss whether the data you are using/curating contains personally identifiable information or offensive content? [N/A]
- 5. If you used crowdsourcing or conducted research with human subjects...
 - (a) Did you include the full text of instructions given to participants and screenshots, if applicable? [N/A]
 - (b) Did you describe any potential participant risks, with links to Institutional Review Board (IRB) approvals, if applicable? [N/A]
 - (c) Did you include the estimated hourly wage paid to participants and the total amount spent on participant compensation? [N/A]

Supplementary Materials for Mining Unseen Classes via Regional Objectness: A Simple Baseline for Incremental Segmentation

Zekang Zhang¹*, Guangyu Gao¹†, Zhiyuan Fang¹, Jianbo Jiao², Yunchao Wei^{3,4}

School of Computer Science, Beijing Institute of Technology
 School of Computer Science, University of Birmingham

1 Details for Reproducibility

Protocols. Here we present more details of the *overlapped* and *disjoint* settings. Specifically, the *overlapped* setting means pixels in samples from \mathcal{D}_t can belong to any classes, including past (step 1 to t-1, formally, $\mathcal{C}_{1:t-1}$), now (\mathcal{C}_t) and future $(\mathcal{C}_{t+1:T})$. Note that only the classes in \mathcal{C}_t would be annotated in \mathcal{Y}_t . Besides, images with multiple classes would appear in several learning steps, with different annotations. The *disjoint* setting, studied by [1, 11], has a non-overlapped $\{\mathcal{D}_t\}$. Thus, each learning step contains a unique \mathcal{D}_t , whose pixels only belong to classes seen in $\mathcal{C}_{1:t-1}$ or in \mathcal{C}_t . It is obvious that *overlapped* setup is more realistic, because *overlapped* has a weaker restriction on data than *disjoint*.

Details of Proposal Reorganization The logits $p \in \mathbb{R}^{N \times |\mathcal{C}|}$ is generated by classification. While proposal $P \in \{0,1\}^{N \times H \times W}$ is a group of binary masks where N is the number of masks and H, W denote height and width. Proposal reorganization is a matrix multiplication of logits and proposal, to obtain probability map of image, with the shape of $|\mathcal{C}| \times H \times W$.

Details of MicroSeg-M. As mentioned in the main paper, MicroSeg-M is an advanced version of MicroSeg by introducing memory sampling strategy from [2]. To be more specific, the strategy is based on random-sampling, and advanced ensuring that there is at least one sample of every seen class in the memory.

2 More Experimental Results and Discussions

Detailed experimental results. Tab. 1 provides experimental results of Pascal VOC 2012 [5] of different incremental scenarios with each class.

Experimental results of disjoint setup. As explained in Sec. 1, disjoint setup is not realistic due to its non-overlapping samples in each learning step. However, we still provide experimental results of the disjoint setup, for a fair comparison with prior works [1, 2, 4, 11]. The result of Tab. 2 shows that our proposed methods, *i.e.*, MicroSeg and MicroSeg-M, outperform the state-of-the-art methods.

³ WEI Lab, Institute of Information Science, Beijing Jiaotong University

⁴ Beijing Key Laboratory of Advanced Information Science and Network zkzhang1998@outlook.com

^{*}Work done during an internship at WEI Lab of Beijing Jiaotong University.

[†]Corresponding author.

Table 1: Detailed experimental results of Pascal VOC 2012 with class.

	bg	aero	bike	bird	boat	bottle	bus	car	cat	chair	cow	table	dog	horse	mbike	person	plant	sheep	sofa	train	TV	mIoU
10-1 (11 steps) MicroSeg MicroSeg-M	89.7 90.9	91.6 86.8	41.2 42.0	95.1 91.5	74.1 78.0	84.4 84.0	90.3 90.9	89.6 87.6	86.8 89.3	37.4 40.1	18.6 68.8	33.4 47.5	75.1 69.4	38.5 40.4	76.6 84.9	87.9 85.7	15.7 34.0	34.1 45.2	28.5 33.6	60.0 70.8	37.0 61.6	61.2 67.8
2-2 (10 steps) MicroSeg MicroSeg-M	85.7 87.2	73.9 72.8	24.4 20.2	40.8 39.2	25.9 34.2	48.8 59.1	27.7 79.5	74.9 82.1	48.0 78.3	4.7 6.6	39.3 35.3	5.1 13.5	54.8 69.4	44.5 47.9	67.1 69.7	80.5 80.1	11.8 25.9	38.0 56.0	27.0 28.1	45.2 70.5	47.0 41.0	43.5 52.2
15-1 (6 steps) MicroSeg MicroSeg-M	89.8 91.2	92.9 93.2	44.4 43.4	95.5 93.1	76.0 78.7	82.8 84.7	92.9 91.9	90.9 91.0	93.4 94.3	48.6 45.8	68.2 88.4	52.9 56.0	89.8 88.5	83.5 84.6	89.7 86.9	90.4 90.1	11.7 22.9	56.2 71.5	24.8 31.0	57.3 71.5	34.2 65.6	69.8 74.4
5-3 (6 steps) MicroSeg MicroSeg-M	89.1 90.9	91.2 81.2	34.8 34.7	89.3 87.8	73.9 67.4	87.3 87.0	82.3 85.0	83.6 78.2	79.6 80.6	4.6 21.8	55.5 55.1	40.0 37.9	76.6 77.3	55.5 52.9	74.1 74.5	87.9 86.2	31.2 43.4	51.4 38.8	30.5 33.8	70.2 74.8	62.7 67.0	64.3 64.6
19-1 (2 steps) MicroSeg MicroSeg-M	88.8 93.6	87.5 86.8	41.4 43.7	92.5 87.5	72.6 73.3	85.3 84.0	96.0 96.1	85.6 90.5	94.9 93.8	36.6 37.3	92.4 87.8	57.6 62.9	90.9 90.4	89.6 88.6	85.0 88.6	89.9 89.9	71.6 71.0	82.2 83.0	50.4 51.5	87.0 85.9	13.9 62.9	75.7 78.5
15-5 (2 steps) MicroSeg MicroSeg-M	91.7 93.0	91.1 91.5	44.8 42.9	92.4 94.0	80.1 80.1	85.2 85.4	93.3 92.2	91.3 91.8	94.5 94.7	43.0 44.5	69.3 89.5	55.9 55.2	90.5 90.1	83.9 87.8	90.1 90.3	90.1 90.5	32.3 48.0	62.3 76.5	30.6 36.1	82.0 77.6	57.0 58.0	73.8 76.6

Table 2: Experimental results on Pascal VOC 2012 for disjoint setup.

Method	VOC	15-1 (6 s	steps)	VOC	19-1 (2	steps)	VOC	15-5 (2 s	steps)
Method	0-15	16-20	all	0-19	20	all	0-15	16-20	all
LwF-MC [9]	4.5	7.0	5.2	63.0	13.2	60.5	67.2	41.2	60.7
ILT [10]	3.7	5.7	4.2	69.1	16.4	66.4	63.2	39.5	57.3
MiB [1]	46.2	12.9	37.9	69.6	25.6	67.4	71.8	43.3	64.7
SDR [11]	59.4	14.3	48.7	70.8	31.4	68.9	74.6	44.1	67.3
PLOP [4]	57.9	13.7	46.5	75.4	38.9	73.6	71.0	42.8	64.3
SSUL [2]	74.0	32.2	64.0	77.4	22.4	74.8	76.4	45.6	69.1
SSUL-M [2]	76.5	43.4	68.6	77.6	43.9	76.0	76.5	48.6	69.8
MicroSeg (Ours)	73.7	24.1	61.9	80.6	16.0	77.4	77.4	43.4	69.3
MicroSeg-M (Ours)	80.0	47.6	72.3	81.1	45.1	79.4	80.7	55.2	74.7
Joint	82.7	75.0	80.9	81.0	79.1	80.9	82.7	75.0	80.9

Further discussion of the proposal. To further investigate the effect of the proposal, we conducted experiments with modified SSUL [2] (a prior work of CISS).

Specifically, SSUL performs the mining of the background by using saliency map [8] as a *saliency detector*, to extract unknown class from background. We complete the experiments on replacing the saliency map with segment proposal and ground truth. The qualitative analysis of these three kinds of "saliency detectors" is shown in Fig. 1. What can be observed is, saliency map only focuses on the most significant areas of the image (*people*), while some areas are missed (*bottle*), proposal tends to focus on more area (*plants*), as the area circled in the Fig. 1. The ground truth (GT), on the other hand, figures out exactly the area that needs to be segmented. Therefore, GT can be considered as the upper bound of quality of the saliency map, because it has complete and precise foreground annotation.

We provide experimental results of VOC 15-1 and VOC 19-1 scenarios in Tab. 3. From the results we can observe that, compared with saliency map, GT can significantly improve the performance of SSUL, while proposal can only slightly improve it. As a saliency detector, *proposal* does not work well compared to *saliency map*. It indicates that the performance improvement of our method comes from neither the information contained in proposal, nor its positive impact on the performance of semantic segmentation only. The key of our proposed method is proposals with the Micro mechanism, trying to solve the problem of background shift in incremental learning.

On the other hand, we further discuss proposals from the perspective of methods of generating them. We have conducted the experiments of replacing proposal generator, including MaskFormer [3] and RPN in Mask R-CNN combined with class-agnostic segmentation head [6, 7] (denote as RPN+Seghead). We also conduct the results for generating different numbers of proposals (N) with Mask2Former. Note that the original setting of MicroSeg is Mask2Former (N=100). All experiments are done in VOC 15-1. As shown in Tab. 4, using other methods as a proposal generator does not significantly affect the performance, comparing to the original setting of MicroSeg. This result further supports our previous claims about proposals.

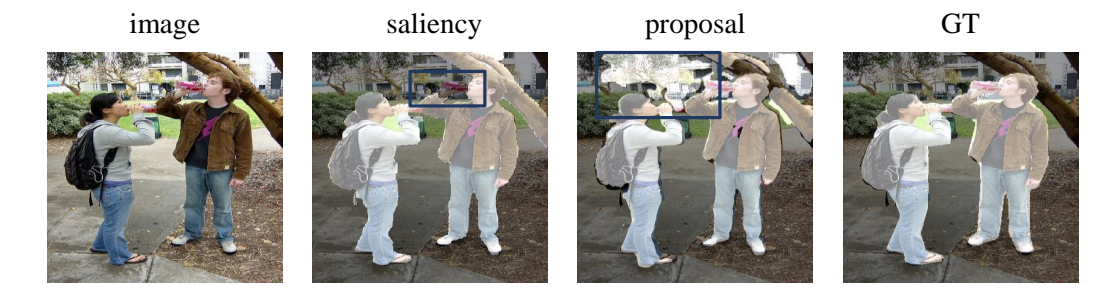


Figure 1: Qualitative comparison of different saliency detector. The boxes point out the main differences among them.

Table 3: Experimental results of SSUL, using different saliency detector. Each row denotes a saliency detector type that SSUL applies: saliency map, saliency proposal and ground truth. The row *saliency map* represents the results of original settings of SSUL. And the following two rows shows the results of SSUL with modified saliency detector. We provide the experimental results of VOC 15-1 and VOC 19-1.

setting	VOC	15-1 (6 s	steps)	VOC	19-1 (2	steps)
setting	0-15	16-20	all	0-19	20	all
saliency proposal	77.3	36.6	67.6	77.7	29.7	75.4
proposal	76.5	38.8	67.5	78.6	35.0	76.6
GT	76.9	46.0	69.7	79.4	65.1	78.8

Table 4: Experimental results of MicroSeg with different proposal generator and different numbers of proposals. We provide the experimental results of VOC 15-1.

cotting	VOC	C 15-1 (6 steps)				
setting	0-15	16-20	all			
RPN+Seghead	80.5	33.0	69.2			
MaskFormer(N = 100)	79.3	34.1	68.5			
Mask2Former(N = 100)(Ours)	80.1	36.8	69.8			
Mask2Former(N = 200)	80.4	37.3	70.1			

Further discussion of the selection of K. Here we will illustrate the reason for K=1 in ADE20K dataset. Hyper-parameter K is the number of future classes. When the prediction of the historical classes is accurate (i.e., high accuracy like 82.7 for VOC 15-1), the remaining uncertainty regions are mainly future classes, and as a result a larger K can better distinguish different future classes. But if the prediction of historical classes is not that accurate (e.g., 43.8 as for the ADE 100-10), many historical classes would be mis-classified and grouped into the remaining future class regions. In this case, if the K is still set to a large value, pixels belonging to the same historical class will be

Table 5: Discussion of K and feature extractor. Using a stronger backbone, a larger K in micro mechanism achieved positive results.

backbone	K	AD 0-15	E 100-10	0 (6 steps) all
ResNet-101	1 2	41.5	21.6 12.4	34.9 31.6 (-3.3)
Swin Transformer	1 2	43.4 43.7	29.6 29.4	38.8 39.0 (+0.2)

forced to be separated into different categories and as a result confuse the model learning. In this case (e.g., on the ADE20K dataset), choice of a smaller K (i.e., K = 1) would be safer and less harmful.

Meanwhile, on the ADE20K dataset, in order to conduct a fair comparison with prior CISS methods [1, 2, 4], we choose to use the ResNet-101 as the backbone. While if we adapt a more advanced model (e.g. the Swin Transformer), a larger K in micro mechanism achieves positive results. The experimental results are provided in Tab. 5.

3 More Qualitative Results

3.1 Qualitative analysis of ADE20K

Fig. 2 shows the qualitative results of the proposed MicroSeg on ADE20K dataset [12] with the 100-10 scenario. Overall, our method performs well in CISS on ADE20K dataset. The first two rows show the ability of the MicroSeg of learning new concepts (*dishwasher* is learned at step 4 and *fan* is learned at step 5). The following two rows show the stability of our method. With the learning step increasing, MicroSeg performs stable predictions. Historical knowledge is not forgotten when learning new concepts. Moreover, for ADE20K, a dense-labeled dataset, both thing and stuff classes are annotated. Our method still achieves well performance at segmenting samples with only stuff classes, *e.g.*, *sky*, *grassland*, *lake*, as shown in the last two rows.

3.2 Extra qualitative results of MicroSeg

We provide extra qualitative results of ADE20K 100-10 and VOC 15-1 in Fig. 3 and Fig. 4.

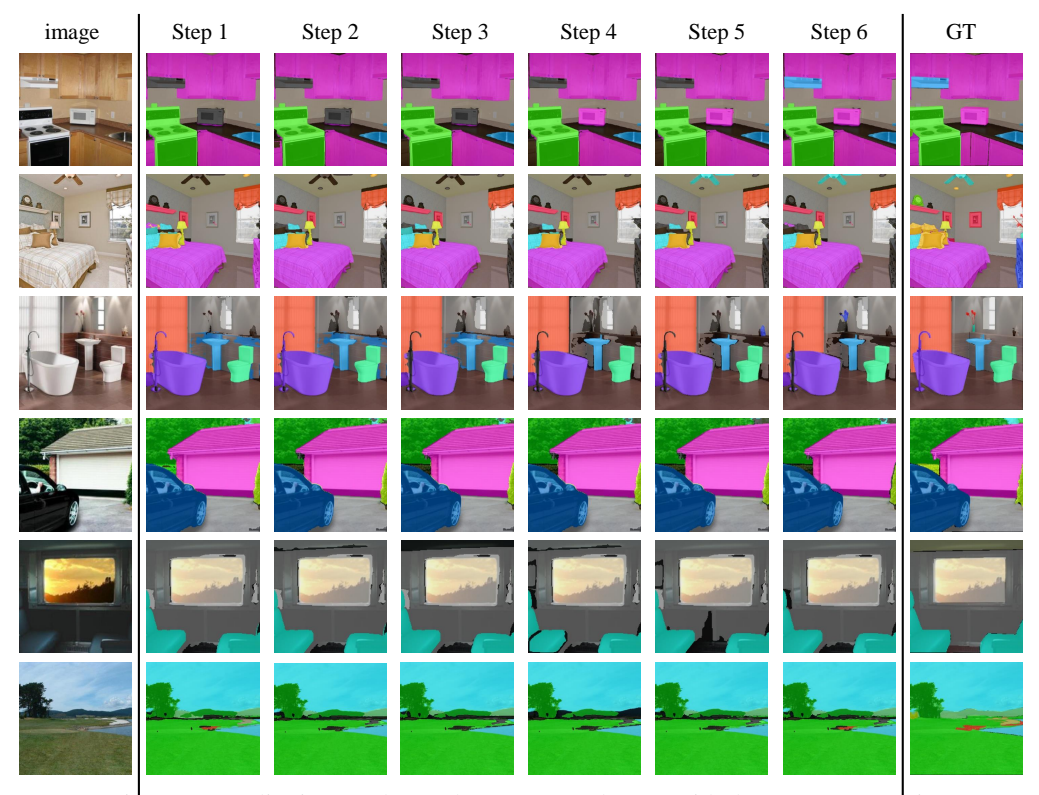


Figure 2: Qualitative results on the ADE20K dataset with the 100-10 scenario.

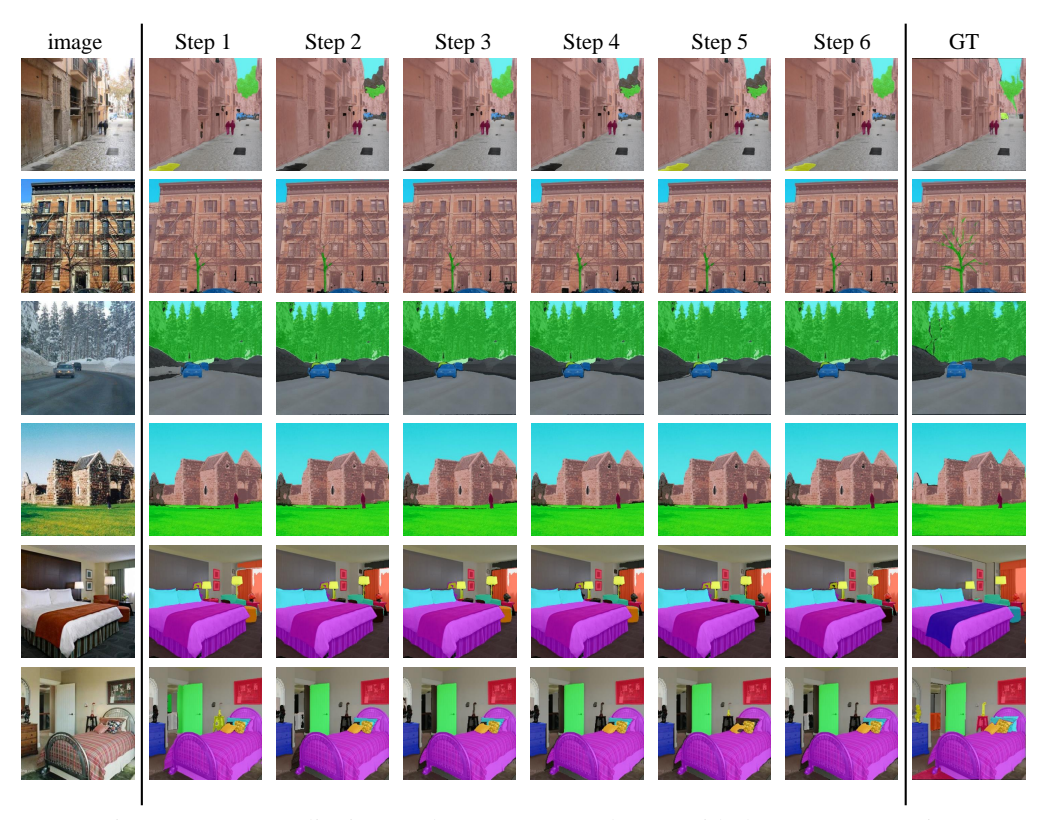


Figure 3: Extra qualitative results on ADE20K dataset with the 100-10 scenario.

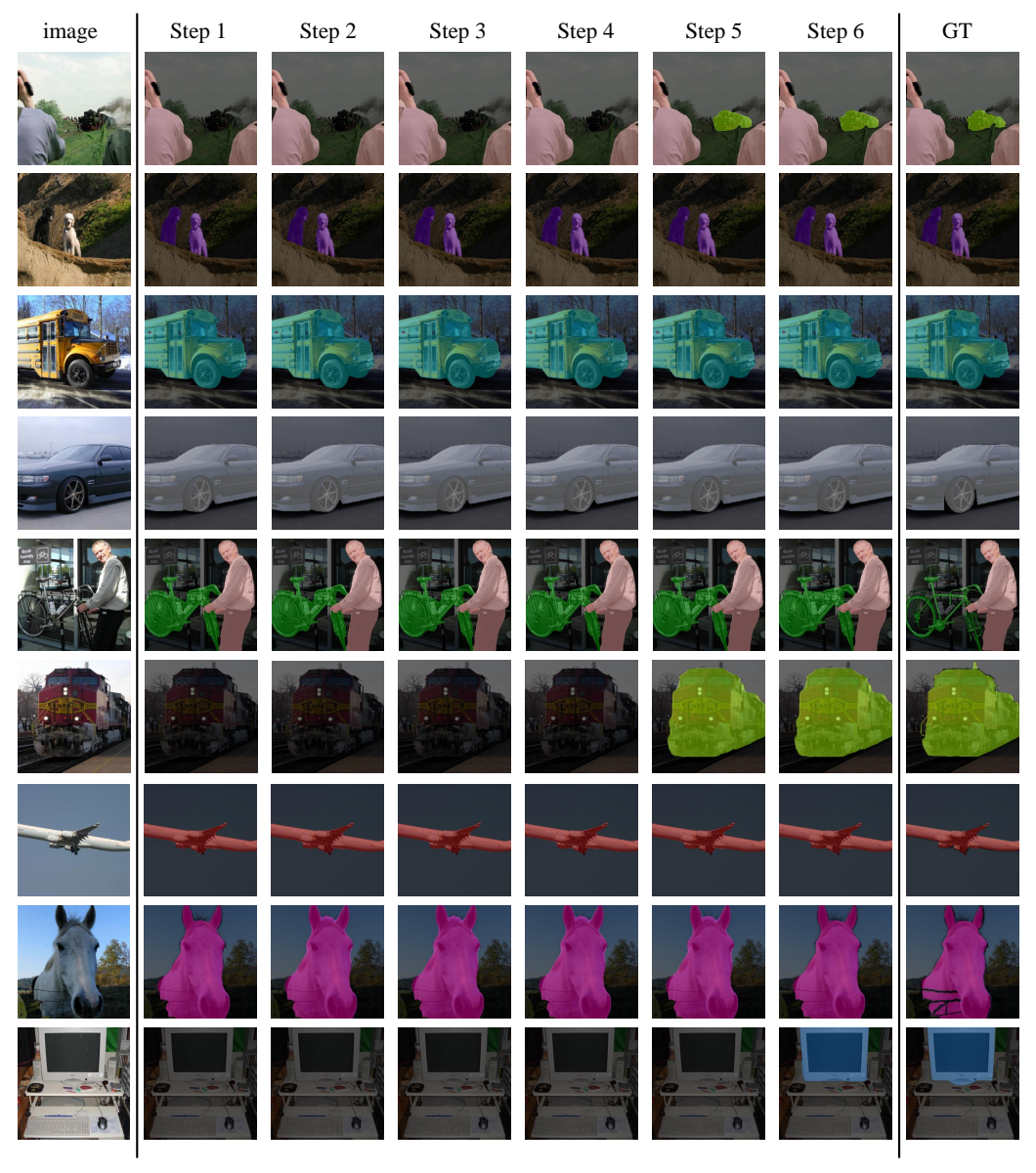


Figure 4: Extra qualitative results on Pascal VOC 2012 dataset with the 15-1 scenario.

References

- [1] Fabio Cermelli, Massimiliano Mancini, Samuel Rota Bulo, Elisa Ricci, and Barbara Caputo. Modeling the background for incremental learning in semantic segmentation. In *Proc. IEEE Conference on Computer Vision and Pattern Recognition*, pages 9233–9242, 2020.
- [2] Sungmin Cha, YoungJoon Yoo, Taesup Moon, et al. Ssul: Semantic segmentation with unknown label for exemplar-based class-incremental learning. *Advances in neural information processing systems*, 34, 2021.
- [3] Bowen Cheng, Alexander G. Schwing, and Alexander Kirillov. Per-pixel classification is not all you need for semantic segmentation. *Advances in neural information processing systems*, 34, 2021.
- [4] Arthur Douillard, Yifu Chen, Arnaud Dapogny, and Matthieu Cord. Plop: Learning without forgetting for continual semantic segmentation. In *Proc. IEEE Conference on Computer Vision and Pattern Recognition*, pages 4040–4050, 2021.
- [5] Mark Everingham, Luc Van Gool, Christopher KI Williams, John Winn, and Andrew Zisserman. The pascal visual object classes (voc) challenge. *International Journal on Computer Vision*, 88(2):303–338, 2010.
- [6] Xiuye Gu, Tsung-Yi Lin, Weicheng Kuo, and Yin Cui. Open-vocabulary object detection via vision and language knowledge distillation. *arXiv preprint arXiv:2104.13921*, 2021.
- [7] Kaiming He, Georgia Gkioxari, Piotr Dollár, and Ross Girshick. Mask r-cnn. In *Proceedings of the IEEE international conference on computer vision*, pages 2961–2969, 2017.
- [8] Huaizu Jiang, Jingdong Wang, Zejian Yuan, Yang Wu, Nanning Zheng, and Shipeng Li. Salient object detection: A discriminative regional feature integration approach. In *Proc. IEEE Conference on Computer Vision and Pattern Recognition*, pages 2083–2090, 2013.
- [9] Zhizhong Li and Derek Hoiem. Learning without forgetting. *IEEE Transactions on Pattern Recognition and Machine Intelligence*, 40(12):2935–2947, 2017.
- [10] Umberto Michieli and Pietro Zanuttigh. Incremental learning techniques for semantic segmentation. In Proc. IEEE International Conference on Computer Vision Workshops, pages 0–0, 2019.
- [11] Umberto Michieli and Pietro Zanuttigh. Continual semantic segmentation via repulsion-attraction of sparse and disentangled latent representations. In *Proc. IEEE Conference on Computer Vision and Pattern Recognition*, pages 1114–1124, 2021.
- [12] Bolei Zhou, Hang Zhao, Xavier Puig, Sanja Fidler, Adela Barriuso, and Antonio Torralba. Scene parsing through ade20k dataset. In *Proc. IEEE Conference on Computer Vision and Pattern Recognition*, pages 633–641, 2017.